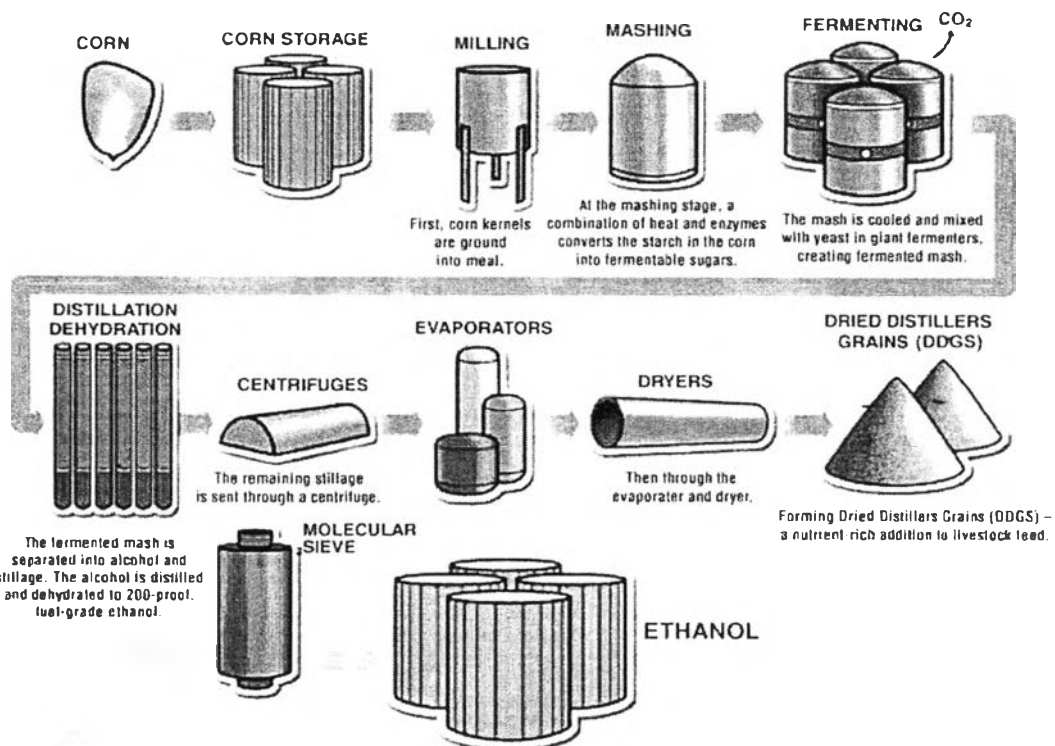


## CHAPTER II

### BACKGROUND AND LITERATURE REVIEW

#### 2.1 Utilization of Bio-ethanol

Bio-ethanol is produced by fermentation process (Figure 2.1). The sources of feedstock can be divided into three types such as sugar based, starch-based and cellulosic-based raw materials (Richard, 2008). Sugar cane, corn crop, and maize are the major raw materials of bio-ethanol production. The main usage of bio-ethanol is to blend with gasoline or to be used instead of gasoline in some types of combustion engine (flex fuel cars). It can be blended at various compositions such as E5 E10 E20 E85 and E100. Brazil is a large consumer and producer of bio-ethanol. It uses E100 for the vehicles in addition to decrease the usage of energy from abroad. Moreover, bio-ethanol can be used to produce the petrochemical feedstock such as paraffins, olefins, and aromatic products.



**Figure 2.1** Commercial ethanol production (dry mill process) (Green Plains Renewable Energy, 2007).

## 2.2 Type of Zeolites

Zeolites are porous materials found in nature such as Chabazite, Analcime, Clinoptilolite or from manmade such as HZSM-5, and SAPO-34. A well-known family of zeolites is aluminosilicate material that contains of tetrahedral silicate ( $\text{SiO}_4$ )<sup>4-</sup> and aluminate ( $\text{AlO}_4$ )<sup>5-</sup>. The unit cell of the zeolite is Sodalite unit that corporates to one another to form the zeolite. Each type of zeolites has the different property, such as channel dimensionality, pore dimensions, as shown in Table 2.1. In petrochemical industry, zeolites are used as catalysts, molecular sieves, and adsorbents or ion-exchange materials.

**Table 2.1** Some types of zeolites and their properties (Meier *et al.*, 2001)

Zeolite	IZA Code	Channel Dimensionality	Channel Type	Pore Dimensions (nm)	SiO <sub>2</sub> /Al <sub>2</sub> O <sub>3</sub> ratio of zeolite in use
Beta	BEA	3D	12	0.76X0.64	27
			12	0.55X0.55	
Y	FAU	3D	12	0.74	30
ZSM-11	MEL	3D	10	0.53X0.54	75
ZSM-5	MFI	3D	10	0.53X0.56	30,80
			10	0.51X0.55	

### 2.2.1 Beta Zeolite

Beta zeolite (HBEA) has a three 3-dimensional structure with 12 ring channel type (Figure 2.2). It has the large pore size along [100] (0.76X0.64 nm). It crystallizes in the P4<sub>1</sub>22 space group, and has the lattice constants: a=12.632, b=12.632 and c=26.168 Å. The channel structure of HBEA is the straight connected pore, and has no pot. HBEA is a good catalyst for acid catalyzed reactions. Paraffins cracking was proposed by Marques *et al.* (2005). They studied the effect of dealuminated of HBEA, and found that dealuminated can decrease the Lewis acid site concentration. So, the main products were C3-C4 alkanes and alkenes. In addition,

toluene alkylation with 1-dodecene and 1-heptene was investigated by Da *et al.* (2001). They proposed that toluene alkylation with 1-dodecene was nearly inactive because of the steric effect of 1-dodecene. However, the obstruction effect in diffusion steps detected in the pore of HBEA leads to increase the selectivity to 2-phenylalkanes (the most biodegradable isomer). The phenol methylation was studied by Sad *et al.* (2010). They compassed that phenol alkylated without significant diffusion restrained on HBEA. Moreover, the selectivity of products is the same as that obtained on HZSM-5. Aromatic acylation was also examined by Heinichen and Holderich (1999). They studied the effect of calcinations and acid treatment, and found that calcinations helped to generate the extra framework alumina species in the micropore. Acid treatment also helped to improve the extra framework of alumina in the outer pore due to the extraction of alumina extra framework out of micropore and due to the formation of silanol groups. So, the main product was larger molecules generated from micropore.

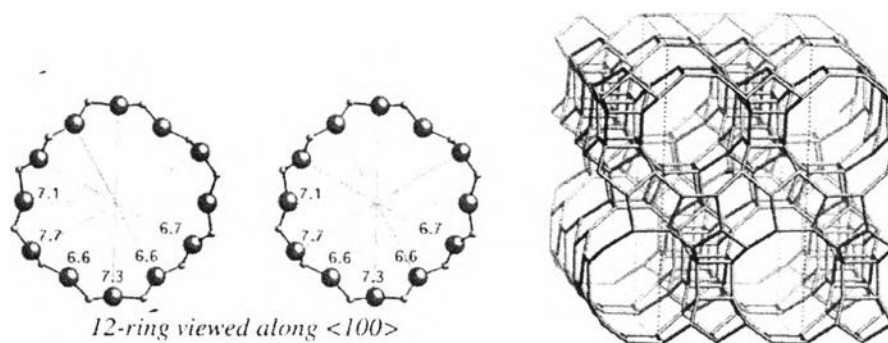


**Figure 2.2** Pore diameter (Å) and a three-dimensional view of beta zeolites framework (Meier *et al.*, 2001).

### 2.2.2 Y Zeolite

Y zeolite (FAU) has a 12 membered-ring structure and it has the large pore size along [111] (7.4 Å) (Figure 2.3) that is proper to a catalytic activity. It crystallizes in the Fd-3m space group, and has the lattice constants:  $a=24.345$ ,  $b=24.345$ , and  $c=24.345$  Å. It can be used in fluid catalytic cracking (FCC) and hydrocracking processes. There are a number of research reports about Y zeolite for

various reactions such as the alkylation of benzene with 1-octene (Craciun *et al.*, 2007). It had two types of products, which are octene isomers and phenyloctane isomers. However, the  $\text{SiO}_2/\text{Al}_2\text{O}_3$  ratio of HY was varied to 12, 26, and 60. The highest  $\text{SiO}_2/\text{Al}_2\text{O}_3$  ratio (60) exhibited the best activity per acid site. Moreover, the oligomerization of ethylene by NiY zeolite was studied by Lallemand *et al.* (2006). The reaction on NiY zeolite exhibited the high activity (16–30 g of oligomers/ $\text{g}_{\text{cat}}\text{h}$ ). The received product was mainly  $\text{C}_4\text{-C}_{12}$  olefin. Methanol dehydration was investigated by Vanoye *et al.* (2013). The conversion at a mild condition ( $T < 250^\circ\text{C}$ ;  $P < 5$  bar) was 27% and 15% for  $\text{SiO}_2/\text{Al}_2\text{O}_3$  ratio = 10.2 and 60, respectively. They mentioned that no correlation between the productivity of the catalyst and concentration of acidic sites could be found.

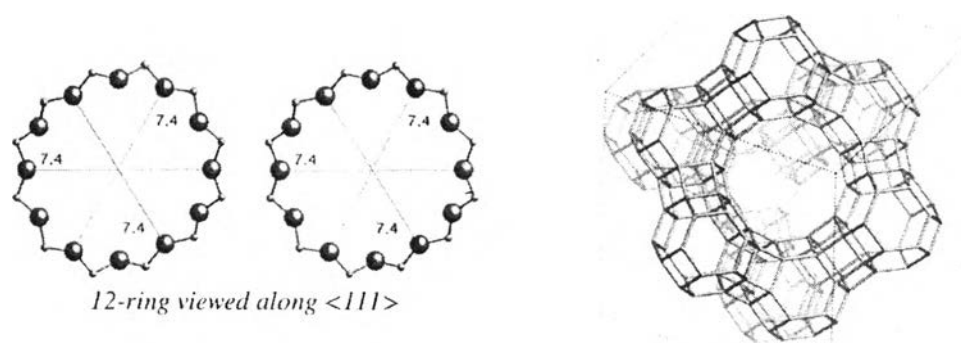


**Figure 2.3** Pore diameter ( $\text{\AA}$ ) and a three-dimensional view of Y zeolite framework (Meier *et al.*, 2001).

### 2.2.3 ZSM-11 Zeolite

HZSM-11 (MEL) has a 10 membered-ring structures with the  $5.3 \times 5.4$   $\text{\AA}$  pore size along  $[100]$  (Figure 2.4). It crystallizes in the  $I-4m2$  orthorhombic space group, and has the lattice constants:  $a=20.27$ ,  $b=19.27$ , and  $c=13.459$   $\text{\AA}$ . There are a few commercial processes that use HZSM-11. In the research field, researchers usually prefer HZSM-11 to HZSM-5 because of their comparable pore sizes but different channel structures. Gu *et al.* (2012) proposed the effect of channel structure

in the dehydration of glycerol. They used HZSM-5, H-Beta, HY, nano HZSM-5, HZSM-11, and nano HZSM-11 as catalysts. Nano HZSM-11 exhibited the excellent catalytic performance of 81.6 mol% glycerol conversion and 74.9 mol% acrolein selectivity. Akhtar *et al.* (2012) showed the aromatization of hexane and propane on Pt doped GaZSM-11. Hexane conversion approached 70.1% over mesoporous Pt/GaZSM-11, as compared with 29.6 and 24.9% for mesoporous and conventional GaZSM-11, respectively. Anunziata *et al.* (1999) worked on the ethane conversion to aromatic hydrocarbons using Mo-MEL zeolite. Ethylene (49% selectivity) was the main product of the ethane aromatization on pure HZSM-11 ( $\text{SiO}_2/\text{Al}_2\text{O}_3 = 54$ ). On the other hand, 2% Mo-ZSM-11 generated the 17.7% benzene and the 18.7% toluene while 2% Mo-SiO<sub>2</sub> almost produced C<sub>9</sub>+ (24.9% selectivity).

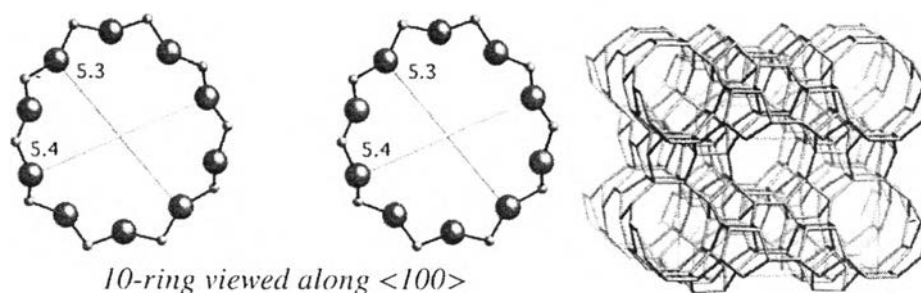


**Figure 2.4** Pore diameter (Å) and a three-dimensional view of ZSM-11 framework (Meier *et al.*, 2001).

#### 2.2.4 ZSM-5 Zeolite

HZSM-5 (MFI) has sinusoidal channel structure of 10 membered ring along the axis [100] (Figure 2.5) direction with the pore size of  $5.1 \times 5.5$  Å. It also has another straight channel structure with 10 membered-ring along the axis [010] with the pore size of  $5.6 \times 5.3$  Å (Meier *et al.*, 2001). It crystallizes in the Pnma orthorhombic space group, and has the lattice constants:  $a=20.1$ ,  $b=19.9$  and  $c=13.4$  Å (Meier *et al.*, 2001). HZSM-5 is a well-known material for various applications such as catalysts, molecular sieve, membrane, and ion exchange resin. There are many research works about ZSM-5 catalysts on such as the methylation of benzene and the aromatization of methanol proposed by Barthos *et al.* (2007). They found

that Mo<sub>2</sub>C/ZSM-5(160) was able to catalyze the methylation of benzene with methanol, which explains the formation of toluene, xylenes, and C<sub>9</sub>+ aromatics in the reaction of methanol. Reddy *et al.* (2012) studied the ethylene conversion and heptanes cracking. The rate of ethylene conversion was found to increase with decreasing ZSM-5 zeolite particle size, while the product distribution was independent of the particle size and morphology of the catalyst. In n-heptanes cracking, the ZSM-5 nanosheet showed lower catalytic activity than particulate ZSM-5, and the distribution of hydrocarbon products was independent of the morphology of ZSM-5. In addition, Ramesh *et al.* (2009) revealed the ethanol dehydration reaction on HZSM-5 at 673K. They investigated that impregnation of H<sub>3</sub>PO<sub>4</sub> on H-ZSM-5 can affect the surface acidity and blockage of the pore. 20% H<sub>3</sub>PO<sub>4</sub> on H-ZSM-5 can give the 64% selectivity of diethyl ether and 35% selectivity of ethylene, and ethanol conversion was 71%. Nevertheless, pure HZSM-5 can produce 15% selectivity of diethyl ether, 79% selectivity of ethylene where as ethanol conversion was 90%.

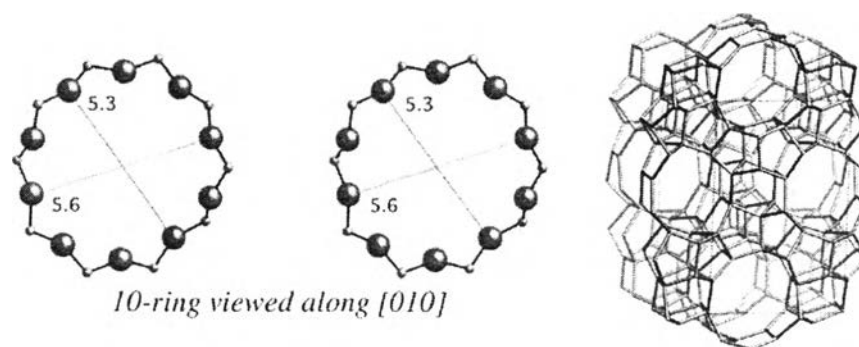


**Figure 2.5** Pore diameter (Å) and a three-dimensional view of ZSM-5 framework (Meier *et al.*, 2001).

### 2.3 Dehydration of Ethanol to Hydrocarbons

Hydrocarbons can be produced alternatively by dehydration process. Inaba *et al.* (2006) showed the mechanism scheme of ethanol dehydration as shown in Figure 2.6. The products are the ethylene and diethyl ether at a high temperature and a low temperature, respectively. Diethyl ether can react further to form C<sub>4</sub> olefins

and both ethylene and C4 olefins can react via oligomerization, aromatization, H-transfer, and cracking to form high molecular weight olefins, paraffins, and BTX. Finally, coke can be generated by carbonization.

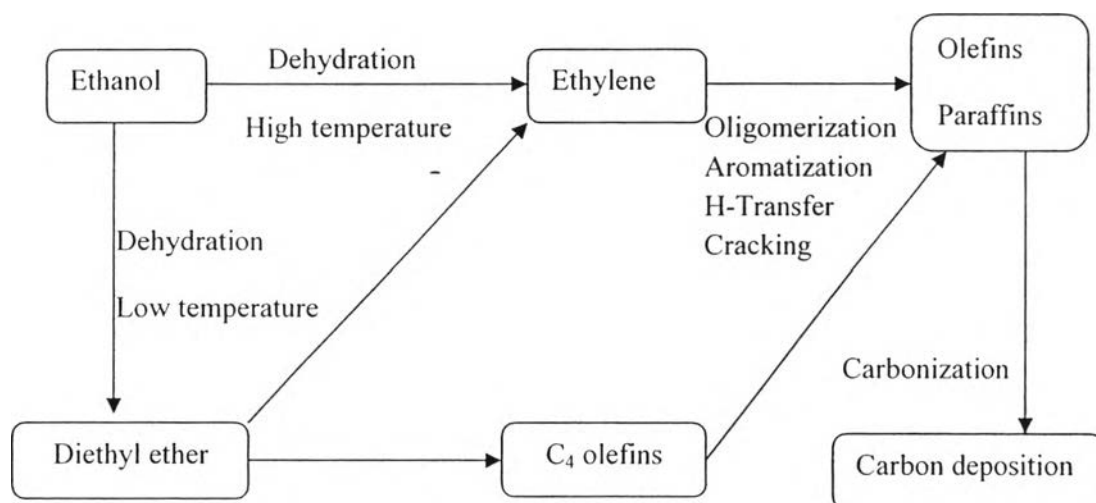


**Figure 2.6** Reaction pathways of ethanol transformation to hydrocarbons.

The dehydration mechanism was proposed via the primary carbocation. The by-product is water and the product is ethylene which can further react to higher olefins, paraffins, or BTX by protonation. The mechanism to convert ethanol to ethylene is showed on Figure 2.7.

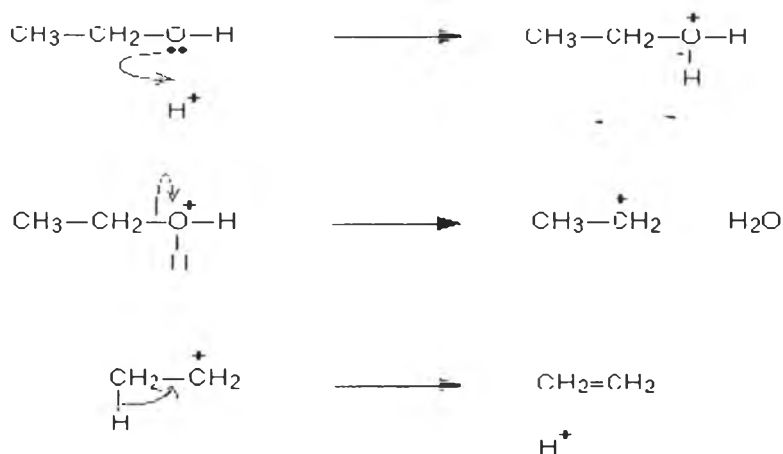


**Figure 2.7** Mechanism of ethanol dehydration to ethylene (Clark, 2013).

The further reaction is the ethylene dimerization reaction to form butene was proposed by Ding *et al.* (2009) that mechanism was shown in Figure 2.8. The further reactions such as aromatization and oligomerization can also take place on acid sites as well.

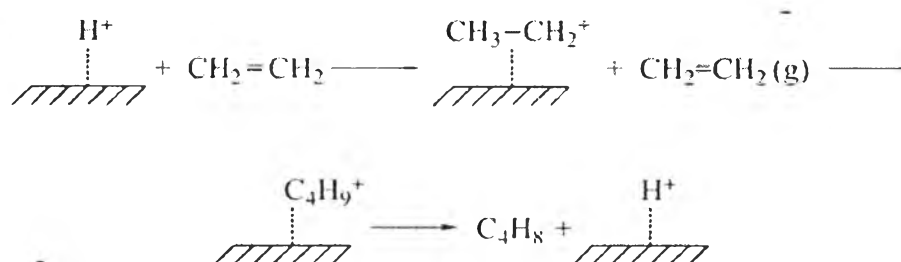


**Figure 2.8** Eley-Rideal mechanism of dimerization of ethylene (Ding *et al.*, 2009).

### 2.3.1 Catalytic Dehydration of Ethanol to Hydrocarbon Gases

Heterogeneous catalysts can be used in the dehydration of ethanol process. Talukdar *et al.* (1997) studied about the ethanol dehydration by using ZSM-5, and they investigated the effects of the  $\text{SiO}_2/\text{Al}_2\text{O}_3$  ratio, %binder ( $\text{Al}_2\text{O}_3$ ), temperature (673K-773K) and ethanol to water ratio in feed. They found that at a high  $\text{SiO}_2/\text{Al}_2\text{O}_3$  ratio, high amounts of C4 olefins and aromatic products were obtained, but the yield of aromatic products decreased with the increase in temperature due to cracking process. The alumina also was known as an ethylene production catalyst because when it mixed with the HZSM-5, the yield of aromatics decreased and the yield of ethylene increased due to the dilution of the Bronsted acid sites. The effect of co-feed water can represent that of the low quality ethanol feed (40-80% diluted with water). At 80% water dilution of feed, 48% ethylene yield was obtained. On the other hand, the yield of liquid product decreased because of the reaction of water with Bronsted acid site.

One of experiments that aimed to yield propylene as the product from ethanol dehydration was from Furumoto *et al.* (2011). They studied the effect of Al, Ga, and Fe incorporated with Si in a zeolite framework by varying the amount of loading of these elements with respect to Si. Furthermore, they varied the ratio of



catalyst to ethanol feeding (W/F). The acid strength and acid amount when Al was replaced by Ga and Fe in the zeolite framework decreased in the order of  $\text{Si(OH)Fe} < \text{Si(OH)Ga} < \text{Si(OH)Al}$ . HZSM-5(Ga) produced mainly ethylene; however, HZSM-5(Al) produced mainly C2-C4 paraffins and C5+. The increasing W/F led to the increase in C2-C4 paraffins and C5+ selectivity, as well. Moreover, they studied the effect of adding P to HZSM-5(Ga), and found that P can suppress the coke formation from 3.0 %w to 1.3%w compared with undoped HZSM-5(Ga), and P can help to maintain the propylene yield at around 28%, as well.

### 2.3.2 Catalytic Dehydration of Ethanol to Liquid Hydrocarbons

Liquid products via ethanol dehydration reaction can be heavy olefins, paraffins, and aromatics. Viswanadham *et al.* (2012) studied the effect of particle size and  $\text{SiO}_2/\text{Al}_2\text{O}_3$  ratio of HZSM-5. They revealed that the aromatic selectivity was increased from 36.3% to 50.6% on the nano-sized particle of HZSM-5 (30 nm) as compared to that observed on the normal particle that has the same acid property. They also found the relationship between aromatization and hydrogen transfer reaction, and suggested that the aromatic products increased along with the decrease of olefins and the increase of paraffins. These occurred only on nano-sized particle. However, the normal particle size in the absence of mesopore can only transform C5+ olefins to propene by cracking reaction, instead of yielding the aromatic product. The nano-sized particle can produce its liquid product in high octane number (>95) that is suitable for gasoline fuel applications.

Furthermore, the effect of type of the zeolite on ethanol dehydration reaction was investigated. Madeira *et al.* (2009) studied the effect of the pore sizes of the HBEA, HFAU, and HMF1 zeolites at 350°C and 30 bars. The zeolites in use had approximately the same Bronsted acid quantity. The conversion of ethanol when ZSM-5 was used as a catalyst still remained at 100%. However, the conversion with using HBEA and HFAU continuously decreased with time-on-stream. HZSM-5 yielded the very few amount of ethylene. On the other side, HFAU and HBEA can produce the ethylene with 80% selectivity, which later decreased gradually with time on stream. HZSM-5 was excellent in producing C3+ hydrocarbons (100% selectivity), and the product was kept nearly constant with time. HBEA and HFAU

can produce 20% C<sub>3</sub>+ hydrocarbons, which subsequently decreased rapidly (2% remaining at 16h time on stream). On the other hand, the C<sub>12</sub>+ hydrocarbons selectivity from HFAU and HBEA was 10% higher than that from ZSM-5(2%) at 0.8h time-on-stream. However, at 10h time-on-stream, the C<sub>12</sub>+hydrocarbons selectivity was diminished. These can be explained by the fast deactivation in HFAU and HBEA, which have the large pore zeolites. Their Bronsted acid sites have been bound with coke, and cannot be active anymore. HZSM-5 has the moderate pore size that was less suffered from coke formation, and it can yield the gasoline product.

Besides the type of zeolite and its pore size, channel structure was also investigated. Gu *et al.* (2012) studied the HZSM-5, H-Beta, HY, nano HZSM-5, HZSM-11, and nano HZSM-11 on glycerol dehydration to acrolein reaction. They found that the nano HZSM-11 showed the best performance in glycerol dehydration to acrolein, which gave 81.6% conversion and 79.4% selectivity to acrolein at 8h time-on-stream. HZSM-11 also gave the great yield of 1-hexene aromatization and isomerization at 370<sup>o</sup>C (Zhang *et al.*, 2010). HZSM-11 showed better performance than HZSM-5 even with less strong acid strength than HZSM-5. The reason is that ZSM-11 has the only straight pore channel; therefore, the product can easily moved out of the pore. At the same particle size and SiO<sub>2</sub>/Al<sub>2</sub>O<sub>3</sub> ratio, the selectivity of aromatics was 70.8% and 78.9% on HZSM-5 and HZSM-11, respectively. Varvarin *et al.* (2013) also studied the effect of pore size and pore structure on n-butanol dehydration to hydrocarbons by using HZSM-5, HZSM-11, H-L, and H-Y zeolites at 250-400<sup>o</sup>C under atmospheric pressure. The difference between the yield of liquid hydrocarbons of HZSM-5 and HZSM-11 is not significant. HZSM-5 and HZSM-11 can produce the aromatic yield of 67 mol% and 62 mol%, respectively at 400<sup>o</sup>C. Moreover, the main products for HL and HY zeolites were alkenes. HL and HY zeolites can give 39 mol% and 34 mol% alkenes yield, respectively.

## 2.4 Group 5A Elements and Their Oxides

Group 5A elements or “*Pnictogens*” include Nitrogen (N), Phosphorus (P), Arsenic (As), Antimony (Sb), and Bismuth (Bi). The properties of group 5A were shown in Table 2.2.

**Table 2.2** Some properties of group 5A elements<sup>1</sup>

General property of the element	N	P	As	Sb	Bi
Atomic number	7	15	33	51	83
Electron configuration	$2s^2 2p^3$	$3s^2 3p^3$	$4s^2 4p^3$	$5s^2 5p^3$	$6s^2 6p^3$
Oxidation state	-3,-2, 1,0,1,2,3, 4,5	-3,0, +3,+4, +5	-3,0, +3,+5	-3,0, +3,+4, +5	-3,0, +3,+5
Atomic radius (pm)	74	110	121	141	152
Ionization energy (kJ mol <sup>-1</sup> )	1403	1060	946	833	703
<sup>2</sup> Electronegativity (kJ mol <sup>-1</sup> )	3.04	2.19	2.18	2.05	2.02
Melting point (K)	63	870	1090	903	545
Boiling point (K)	77	704	886	1850	1900
$\Delta H_{f(\text{atom})}$ (kJ mol <sup>-1</sup> )	476	334	289	259	207

<sup>1</sup> (Ratananukul and Tuntulani, 2006)

<sup>2</sup> (Allen, 1989)

<sup>3</sup> (Satake and Iqbal, 1995)

The oxidation state of group 5A elements can indicate the acidic property of their oxides, which can be roughly measured by the difference of electronegativity between oxygen and the metal, semi-metal, or non-metal. The more electronegativity of metal, semi-metal, or non-metal is different from that of oxygen (electronegativity of oxygen = 3.44), the less acid property is obtained.

There are some suggestions of acid property of some oxide compounds as shown in Figure 2.9. For the group 5A oxides in the highest oxidation number, the acid character increases along the column of the table (Satake and Iqbal, 1995).

	B <sub>2</sub> O <sub>3</sub>	CO <sub>2</sub>	N <sub>2</sub> O <sub>5</sub>		F <sub>2</sub> O
	Al <sub>2</sub> O <sub>3</sub>	SiO <sub>2</sub>	P <sub>2</sub> O <sub>10</sub>	SO <sub>2</sub>	Cl <sub>2</sub> O
	Ga <sub>2</sub> O <sub>3</sub>	GeO <sub>2</sub>	As <sub>2</sub> O <sub>5</sub>	SeO <sub>3</sub>	Br <sub>2</sub> O
	In <sub>2</sub> O <sub>3</sub>	SnO <sub>2</sub>	Sb <sub>2</sub> O <sub>5</sub>	TeO <sub>3</sub>	I <sub>2</sub> O <sub>5</sub>
	Tl <sub>2</sub> O <sub>3</sub>	PbO <sub>2</sub>	Bi <sub>2</sub> O <sub>5</sub>		

**Figure 2.9** Acid property of some oxide substances (Satake and Iqbal, 1995).

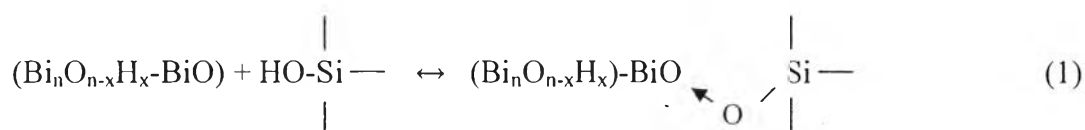
## 2.5 Activity of Group 5A Elements

The uses of the group 5A element in many reactions have been revealed by many researchers. Takahashi *et al.* (2012) studied the effect of P content added in ZSM-5 on the dehydration of ethanol to propylene at 550°C, and they found that adding P in the amount of P/Al < 0.5 can enhance the propylene selectivity. At P/Al = 0.5, the yield of propylene reached the maximum of 30.5% because the phosphorus can partially decrease the strong acid strength. However, at P/Al > 0.5, the acid density also decreased and nearly disappeared at P/Al = 1.

On the other hand, arsenic is the toxic substance, so it is not usually used in any application. Antimony (Sb) is an element that is usually used as a catalyst in many reactions. Zaitseva and Gushikem (2002) revealed that Sb<sub>2</sub>O<sub>5</sub> in the system of SiO<sub>2</sub>/ZrO<sub>2</sub>/Sb<sub>2</sub>O<sub>5</sub> showed the acidic property. The set of catalyst exhibited the transmittance bands at 1,445, 1,457, 1,491, and 1,545 cm<sup>-1</sup> at the temperatures of 323-573 K. The peak at 1,445 cm<sup>-1</sup> represented the hydrogen bonding between Sb<sub>2</sub>O<sub>5</sub> and ≡Si-OH. Moreover, 1,457 cm<sup>-1</sup> is the peak of Lewis acid site that appeared at 373K, but the peak at 573K completely disappeared due to the highly disperse coordinative unsaturated Sb(V) on the surface. This peak evolved only in the system of SiO<sub>2</sub>/ZrO<sub>2</sub>/Sb<sub>2</sub>O<sub>5</sub> and SiO<sub>2</sub>/ZrO<sub>2</sub> but it did not appear for bulk Sb<sub>2</sub>O<sub>5</sub> and SiO<sub>2</sub>. The peak at 1,545 cm<sup>-1</sup> represented the Bronsted acid site. This peak still unchanged

through 573K. The peak of the bulk  $\text{Sb}_2\text{O}_5$  disappeared at 573K because the solid easily dehydrates, and the Bronsted acid site disappeared.

Bismuth oxide has been studied by Dumitriu *et al.* (2003). They incorporated Bi in the framework of the ZSM-5 and compared the catalyst with that prepared by impregnation method on aromatic oxidation by  $\text{H}_2\text{O}_2$ . They found that the Bi catalyst exhibited the Lewis acid site at unsaturated cation framework, and exhibited the Bronsted acid site at the  $\text{Bi}\cdots\text{O}-\text{Si}$  linkage. The pyridine adsorption test revealed that Bi can improve the acid property of ZSM-5 (Table 2.3). The reaction between bismuth compound and ZSM-5 was exhibited in the reaction Scheme (1). Furthermore, they also concluded the content of Bi and the crystal size affected the Bronsted acid property.



Moreover, they revealed that the impregnation of Bi decreased more surface area and pore volume than the incorporated Bi in the framework. However, at the 6.63% content of Bi, Bi formed the extra framework crystalline phase. Moreover, the result from  $\text{CO}_2$  adsorbed IR spectroscopy showed that Bi-incorporated ZSM-5 did not have the peak at  $1200\text{-}1700\text{ cm}^{-1}$ , so they do not have the basic site.

**Table 2.3** Absorbance of pyridine species adsorbed on Bronsted (py-B) and Lewis acid sites (py-L) at  $150\text{ }^\circ\text{C}$  (Dumitriu *et al.*, 2003)

Sample	py-B (absorbance/g)	py-L (absorbance/g)
H-ZSM-5	10	4.2
Na-ZSM-5	0	4.3
Bi4.26	3.9	4.2
Bi5.54	6.3	6.7
Bi6.64	3.1	10.1

### 2.5.1 Activity of Group 5A Elements in Improvement of Aromatic

#### Hydrocarbon

The improvement of the aromatic product was revealed by Pasomsub (2013). He studied the ZSM-5 incorporated with group 5A oxides in the highest oxidation state ( $X_2O_5$  where X is P, Sb, or Bi) at 1%, 2%, 3%, and 4% loading can improve the xylene, ethyl benzene, C9 and C10+ aromatic yields. However, when  $P_2O_5$  was added to ZSM-5, the formation of p-xylene, ethylbenzene, C9 and C10+ aromatics increased while that of benzene, toluene, and m-xylene decreased. The p-xylene reached the maximum at 3% $P_2O_5$  loading on HZSM-5. The yield of oil decreased with the increased loading of  $P_2O_5$ , opposite to the yield of gas. The gaseous products mainly consisted of ethylene and C3 hydrocarbons. The ethylene product tended to increase; however, C3 hydrocarbons tended to decrease with the increased loading amount of  $P_2O_5$  on HZSM-5. In addition, 2% $Sb_2O_5$  on HZSM-5 can produce the maximum oil yield.  $Sb_2O_5$  on HZSM-5 can suppress toluene, benzene, and m-xylene formation. The selectivity of ethylbenzene can reach the maximum at 1% loading of  $Sb_2O_5$  on HZSM-5. The gasoline range product decreased with the increasing loading on HZSM-5, whereas the kerosene range product increased with the increasing amount of  $Sb_2O_5$  loading. The gaseous C3 hydrocarbons also decreased with the increasing loading of  $Sb_2O_5$ . On the other hand, ethylene selectivity increased with the increasing loading of  $Sb_2O_5$ .  $Bi_2O_5$  on HZSM-5 showed the same trend as  $P_2O_5$  and  $Sb_2O_5$  in terms of suppressing the benzene and toluene selectivities and improving the C9 and C10+ aromatics. Xylene selectivity decreased with the increasing  $Bi_2O_5$ , which was different from that of  $P_2O_5$  and  $Sb_2O_5$  on HZSM-5. From the aforementioned,  $P_2O_5$ ,  $Sb_2O_5$ , and  $Bi_2O_5$  can improve the acid property of HZSM-5, leading to the increases in the C9 and C10+ formation and the suppression of m-xylene, toluene and benzene selectivities at the same time. However,  $P_2O_5$ /HZSM-5 showed the great yield of C9 aromatics than that of C10+ aromatics because their moderate acid strength that cannot further protonate to C10+ aromatics. The gaseous product mainly consisted of ethylene and C3 hydrocarbons. C3 hydrocarbons usually further cracks to a lighter molecule (such as ethylene) or reacts to a larger molecule (such as aromatic products).

In addition, Wongwanichsin (2013) studied the antimony oxide at 3, and 5% loading on SAPO-34. He found that 5% loaded antimony oxide ( $\text{Sb}_2\text{O}_3$ ) can give 77.5% selectivity of C10+ aromatics while the unloaded SAPO34 did not produce the C10+ aromatic product. For the analysis of petroleum fractions, 5%  $\text{Sb}_2\text{O}_3$  on SAPO-34 also produced 97.1% selectivity of gasoline range product while the unloaded SAPO-34 did not produce any liquid product.

In conclusion, the improvement of the p-xylene, ethylbenzene, C9 and C10+ aromatic selectivities was expected to be accomplished by incorporation of oxides with a larger pore size zeolite than HZSM-5. HBEA and HY are large pore size zeolites that have the potential to produce high molecular weight molecules of hydrocarbons. Moreover, the group 5A oxides are the acidic oxide. However, in some literature reviews, the decrease of Bronsted acid site of zeolite resulted in a higher aromatic production. So, whether or not the oxides of group 5A (P, Sb, and Bi) doped on HBEA and HY can improve the p-xylene, ethylbenzene, C9 and C10+ aromatics, or longer chain hydrocarbons was investigated. Moreover, HZSM-11, with the straight channel structures, has been reported to improve the aromatic product in 1-hexene aromatization and isomerization, glycerol dehydration to acrolein, and n-butanol dehydration. So, the ethanol dehydration over HZSM-11 is attractive to investigation. In addition, HZSM-11 promoted with the oxides of group 5A (P, Sb, and Bi) was also investigated whether or not it can improve the formation of larger hydrocarbons than the kerosene range.